JPL D-1000784

Surface Biology and Geology (SBG) Observing Terrestrial Thermal Emission Radiometer (OTTER)

Level 2 Cloud Mask Algorithm Theoretical Basis Document (ATBD)

Version 0.5
June 24, 2023

Glynn Hulley
Jet Propulsion Laboratory
California Institute of Technology

JPL D-1000784

National Aeronautics and
Space Administration

Jet Propulsion Laboratory
4800 Oak Grove Drive
Pasadena, California 91109-8099
California Institute of Technology

This research was carried out at the Jet Propulsion Laboratory, California Institute of Technology, under a contract with the National Aeronautics and Space Administration.

Change History Log

Revision	Effective Date	Prepared by	Description of Changes
V0.5	09/20/2023	Glynn Hulley	SBG L2 CLOUD ATBD first draft.

Contacts

Readers seeking additional information about this study may contact the following:

Glynn C. Hulley

MS 183-501
Jet Propulsion Laboratory
4800 Oak Grove Dr.
Pasadena, CA 91109
Email: *glynn.hulley@jpl.nasa.gov*
Office: (818) 354-2979

SBG Science Team

Team members:

Abstract

The 2017-2027 Decadal Survey for Earth Science and Applications from Space (ESAS 2017) was released in January 2018. ESAS 2017 was driven by input from the scientific community and policy experts and provides a vision and strategy for Earth observation that informs federal agencies responsible for the planning and execution of civilian space-based Earth-system programs in the coming decade, including the National Aeronautics and Space Administration (NASA), the National Oceanic and Atmospheric Administration (NOAA), and the U.S. Geological Survey (USGS). NASA has, thus far, utilized this document as a guide to inform exploration of new Earth mission concepts which are later considered as candidates for fully funded missions. High-priority emphasis areas and targeted observables include global-scale Earth science questions related to hydrology, ecosystems, weather, climate, and solid earth. One of the Designated Observables (DO's) identified by ESAS 2017 was Surface Biology and Geology (SBG) with a goal to acquire concurrent global hyperspectral visible to shortwave infrared (VSWIR; 380–2500 nm) and multispectral midwave and thermal infrared (MWIR: 3–5 μm; TIR: 8–12 μm) imagery at high spatial resolution (~30 m in the VSWIR and ~ 60 m in the TIR) and sub-monthly temporal resolution globally. The final sensor characteristics will be determined during the mission formulation phase, but ESAS 2017 provides guidance for a VSWIR instrument with 30–45 m pixel resolution, ≤16 day global revisit, SNR > 400 in the VNIR, SNR > 250 in the SWIR, and 10 nm sampling in the range 380–2500 nm. It also recommends a TIR instrument with more than five channels in 8–12 μm, and at least one channel at 4 μm, ≤60 m pixel resolution, ≤3 day global revisit, and noise equivalent delta temperature (NEdT) ≤0.2 K (NASEM, 2018; Schimel et al., 2020). Alone, SBG will provide a comprehensive monitoring approach globally. Complemented with systems like Landsat and Sentinel-2, global change processes with faster than 16-day global change rates can be mapped—at lower spectral resolution—but high temporal revisit.

Contents

Figures

Tables

1 Introduction

The Surface Biology and Geology (SBG) thermal infrared (TIR) instrument – termed the Observing Thermal Emission Radiometer (OTTER) consists of a TIR multispectral scanner with six spectral bands operating between 8 and 12.5 µm and two mid-infrared (MIR) bands at 4 µm and 4.8 µm, with a 60 m ground sample distance (GSD), 3 day global revisit, and noise equivalent delta temperature (NEdT) ≤0.2 K (NASEM, 2018; Schimel et al., 2020). Table 1 shows the SBG instrument characteristics relative to current TIR sensors. The TIR data will be acquired at a spatial resolution of 60m x 60m with a swath width of 935 km (60°) from an altitude of ~700 km. This document outlines the theory and methodology for generating the OTTER Level-2 (L2) cloud mask product (SBGCLOUD). The algorithm for SBGCLOUD will be based on a statistical-based confidence level approach with clear-sky TIR brightness temperature look up tables. The thresholds are dynamically interpolated based on time of day, month of year, and location to take into account changes in the land surface emissivity, atmospheric conditions and seasonality.

Discriminating clouds is a challenging endeavor and depends on not only the type of cloud being detected, but also the type of surface over which the cloud is detected. Clouds are brighter and colder than the land surface they obscure and these properties can be exploited with the SBG high spatial resolution TIR bands. Cloud and land surface variability, however, creates ambiguity in cloud screening. A cloud signature that works well for one scene may be ineffective for another, depending on the land surface type. Accurate cloud identification is also affected by surface features such as snow, ice, and reflective sand that have reflectance signatures similar and in some cases identical to clouds in the visible bands, especially at higher elevations.

Table 1: SBG measurement characteristics as compared to other spaceborne TIR instruments.

Instrument	**Platform**	**Resolution (m)**	**Revisit (days)**	**Daytime overpass**	**TIR bands (8-12.5 μm)**	**Launch year**
OTTER	SBG	60	3	12:30 pm	6	2028*
ECOSTRESS	ISS	38 × 68	3-5	Multiple	5	2018
ASTER	Terra	90	16	10:30 am	5	1999
ETM+/TIRS	Landsat 7/8	60-100	16	10:11 am	1/2	1999/2013
VIIRS	Suomi-NPP	750	Daily	1:30 am/pm	4	2011
MODIS	Terra/Aqua	1000	Daily	10:30/1:30 am/pm	3	1999/2002
GOES	Multiple	4000	Daily	Every 15 min	2	2000

For these reasons, the SBG cloud mask includes a confidence level mask that classifies pixels as follows (0 = confident cloudy, 1 = probably cloudy, 2 = probably clear, and 3 = confident clear).

The remainder of the document will discuss the SBG instrument characteristics, provide a background on cloud detection algorithms, and show some examples of the SBG cloud detection algorithm (SBGCLOUD).

2 SBG Instrument Characteristics

2.1 Band positions

The TIR instrument will acquire data from a sun-synchronous orbit of 700 km with 60m spatial resolution in eight spectral bands located in the MIR (2) and TIR (6) part of the electromagnetic spectrum between 4 and 12.5 µm shown in Figure 1. The center position and width of each band is provided in Table 2. The positions of three of the TIR bands closely match the first three thermal bands of ASTER, while two of the TIR bands match bands of ASTER and MODIS typically used for split-window type applications (ASTER bands 12–14 and MODIS bands 31, 32). It is expected that small adjustments to the band positions will be made based on ongoing engineering filter performance capabilities.

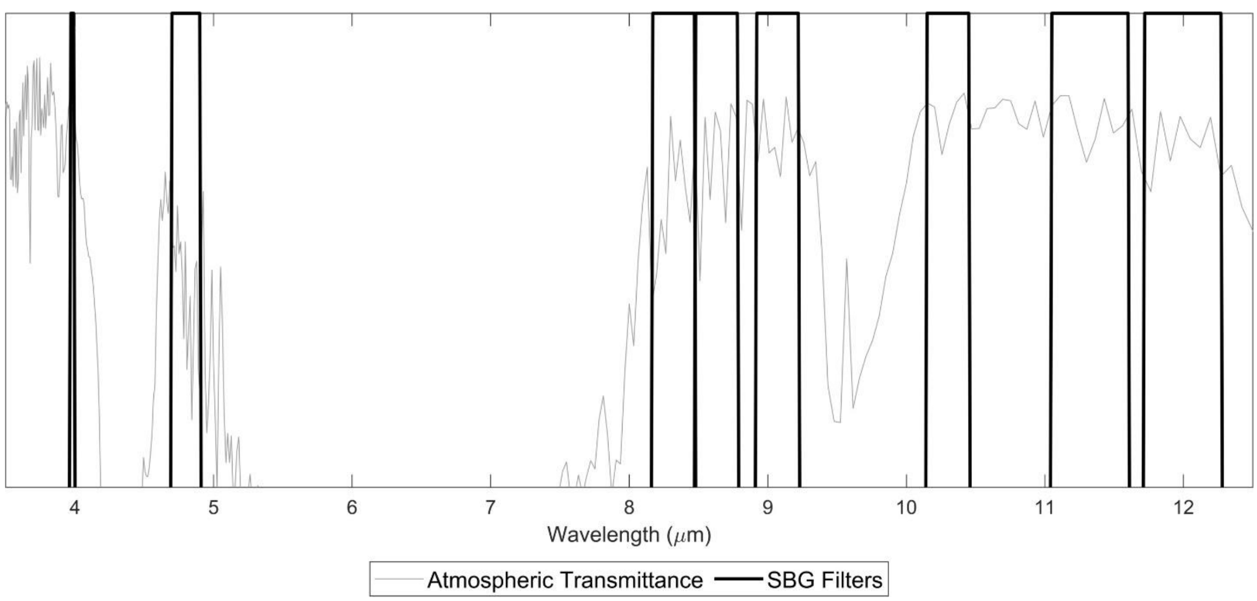

Figure 1: SBG boxcar filters for two MIR bands and six TIR bands from 3.8-12.5 microns with a typical atmospheric transmittance spectrum in gray highlighting the atmospheric window regions. Note the spectral width and location of the filters are finalized (see Table 2), however the spectral shape will be determined when the detectors are fabricated.

Table 2: SBG final band positions and characteristics.

Band #	Center Wavelength (μm)	Spectral Width (FWHM) (nm)	Tolerance Center Wavelength (± nm)	Tolerance Spectral Width (±nm)	Knowledge Center Wavelength (±nm)	Knowledge Spectral Width (±nm)	Accuracy (Kelvin)	NEdT (Kelvin)	Range (Kelvin)
MIR-1	3.98	20 (TBC)	50	10	10	10	≤3@750	≤0.3@750	700-1200
MIR-2	4.8	150 (TBC)	100	50	20	20	≤1@450	≤0.2@450	400-800
TIR-1	8.32	300 (TBC)	100	50	20	20	≤0.5@275	≤0.2@275	200-500
TIR-2	8.63	300 (TBC)	100	50	20	20	≤0.5@275	≤0.2@275	200-500
TIR-3	9.07	300 (TBC)	100	50	20	20	≤0.5@275	≤0.2@275	200-500
TIR-4	10.30	300 (TBC)	50	50	20	20	≤0.5@275	≤0.2@275	200-500
TIR-5	11.35	500 (TBC)	100	50	20	20	≤0.5@275	≤0.2@275	200-500
TIR-6	12.05	500 (TBC)	100	50	20	20	≤0.5@275	≤0.2@275	200-500

The TIR instrument will operate as a push-whisk mapper very similar to SBG with 256 pixels in the cross-whisk direction for each spectral channel (Figure 2), which enables a wide swath and high spatial resolution. As the spacecraft moves forward, the scan mirror sweeps the focal plane ground projection in the cross-track direction. Each sweep is 256-pixels wide. The different spectral bands are swept across a given point on the ground sequentially. From the spacecraft altitude of 665 km, the resulting swath is 935 km wide. The scan mirror rotates at a constant angular speed and sweeps the focal plane image 68.8° across nadir, then to two on-board blackbody targets at 300 K and 340 K. Both blackbodies will be viewed with each cross-track sweep every 1.29 seconds to provide gain and offset calibrations.

2.2 Radiometer

[Updated info here on radiometer]

Table 3: SBG TIR Instrument and Measurement Characteristics

Spectral	
Bands (µm)	4, 4.8, 8.32, 8.63, 9.07, 10.3, 11.35, 12.05
Bandwidth (nm)	20, 150, 300, 300, 300, 300, 500, 500
Accuracy at 300 K	<0.01 µm
Radiometric	
Range	TIR bands (200 - 500 K) 4 micron band (700 -1200 K) 4.8 micron band (400 - 800 K)
Resolution	< 0.05 K, linear quantization to 14 bits
Accuracy	< 0.5 K 3-sigma at 275 K
Precision (NEdT)	< 0.2 K
Linearity	>99% characterized to 0.1 %
Spatial	
IFOV	60m
MTF	>0.65 at FNy
Scan Type	Push-Whisk
Swath Width at 665-km altitude	935 km (+/- 34.4°)
Cross Track Samples	10,000 (check)
Swath Length	
Down Track Samples	256
Band to Band Co-Registration	0.2 pixels (12 m)
Pointing Knowledge	10 arcsec (0.5 pixels) (approximate value, currently under evaluation)
Temporal	
Orbit Crossing	Multiple
Global Land Repeat	Multiple
On Orbit Calibration	
Lunar views	1 per month {radiometric}
Blackbody views	1 per scan {radiometric}
Deep Space views	1 per scan {radiometric}
Surface Cal Experiments	2 (day/night) every 5 days {radiometric}
Spectral Surface Cal Experiments	1 per year
Data Collection	
Time Coverage	Day and Night
Land Coverage	Land surface above sea level
Water Coverage	n/a
Open Ocean	n/a
Compression	2:1 lossless

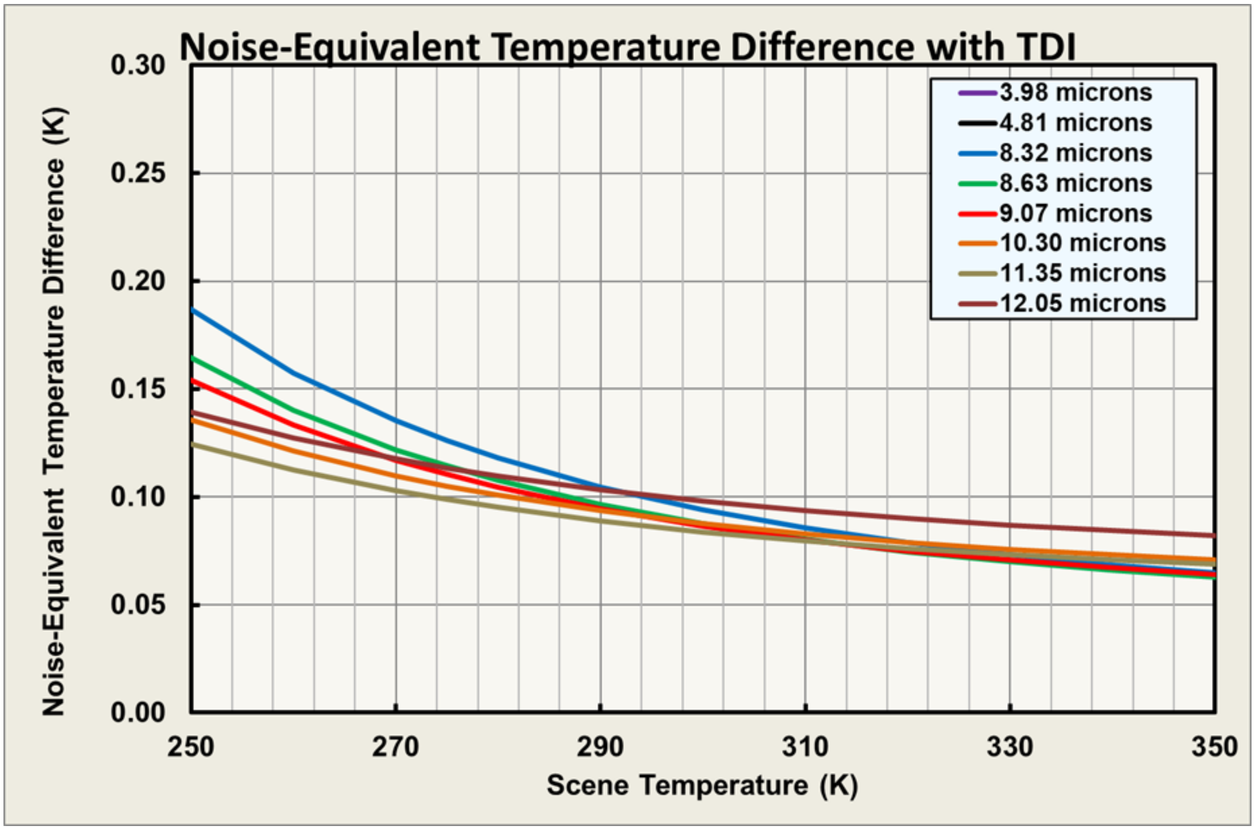

Figure 2: Modeled SBG NEdT versus scene temperature for the two MIR and six TIR bands with time delay integration (TDI).

3 Theory and Methodology

3.1 Objectives

The cloud mask generated from the SBGCLOUD algorithm will indicate whether a given view of the earth surface is unobstructed by clouds. The cloud mask will be generated at native SBG spatial resolution (nominally 60m). Input to the SBGCLOUD algorithm is assumed to be calibrated and geolocated L1B TIR brightness temperature data. The cloud mask will be determined for good data only (i.e., fields of view where data in SBG TIR bands have radiometric integrity). Several points need to be made regarding the approach to the SBG cloud mask presented in this Algorithm Theoretical Basis Document (ATBD).

(1) The cloud mask confidence level flags will be distributed as a separate additional L2 product, which investigators can use to screen data as appropriate for their studies, however a final cloud mask will be included with the L2 LST&E product for users who wish to use the standard confidence levels (cloud = confident + probably cloudy pixels).

(2) The cloud mask ATBD assumes that calibrated, quality controlled TIR data are the input and a cloud mask is the output.

(3) In certain heavy aerosol loading situations (e.g., dust storms, volcanic eruptions, and forest fires) the cloud mask may flag the aerosol-laden atmosphere as cloudy.

The cloud mask products will include a confidence level mask (0 = confident cloudy, 1 = probably cloudy, 2 = probably clear, and 3 = confident clear) and a final cloud mask (1 = cloud, 0 = clear) based on a combination of the confidence flags and digital elevation model (see Table 4). In summary, our approach to the SBG cloud mask is, in its simplest form, to provide a binary confidence level output for each pixel, and a final cloud mask based on standard processing approach.

3.2 Background

The SBG cloud mask will use a very similar approach as the ECOSTRESS TIR-only band cloud mask that is based on a dynamic threshold approach (or Bayesian classification scheme) used for the Advanced Along Track Scanning Radiometer (AATSR) (Bulgin et al. 2014; Merchant et al. 2014), and its successor the Sea and Land Surface Temperature Radiometer (SLSTR). The algorithm derives the pixel-level cloud mask using a combination of TIR simulated clear-sky brightness temperatures that are interpolated from Look Up Tables (LUT) onto the satellite scene, and is valid both day and night.

3.3 Brightness temperature calculation

Theoretically, brightness temperatures for each SBG band can be calculated on a pixel-by-pixel basis by inverting the Planck equation:

$$T_b(\lambda) = \frac{c2}{\lambda \cdot \ln\left(\frac{c1}{\lambda^5 \cdot \pi \cdot L_\lambda} + 1\right)} \tag{1}$$

where: λ is wavelength in µm, $c1$ = 0.0143877, $c2$ = 3.741775e-22, L_λ is the at-sensor spectral radiance in $W/(m^2 \cdot sr \cdot \mu m)$

However, this formulation will increasingly become inaccurate for a sensor's spectral response that deviates from delta function behavior. Instead, we use a look up table (LUT) approach in which the Planck function is used to compute expected radiances for each respective SBG band's spectral response functions over a range of temperatures in 0.01 K intervals that encompass the full range of expected Earth-like temperatures (typically 150 to 380 K). This results in a table of values of radiances versus temperatures for each given sensor. The table can then simply be 'inverted' by interpolating to get the desired temperature. The table can be modified to any desired precision by decreasing the step size interval (e.g. from 0.01 to 0.001 K).

4 Cloud mask implementation

4.1 Brightness temperature LUT interpolation and thresholding

The expected clear-sky brightness temperatures are simulated using forward calculations from the RTTOV-12 radiative transfer model with input atmospheric profile information from the GEOS5-FP product (GMAO) on 0.25×0.25° grids combined with surface emissivity from the Combined ASTER MODIS Emissivity for Land (CAMEL) v2 product (Borbas et al. 2018; Feltz et al. 2018). For each month of simulations and for each 6hr period, a statistical distribution of the clear-sky brightness temperatures for each grid cell location is used to determine the three confidence level thresholds (Q1, Q2, Q3) using an interquartile range (IQR) approach (Figure 7).

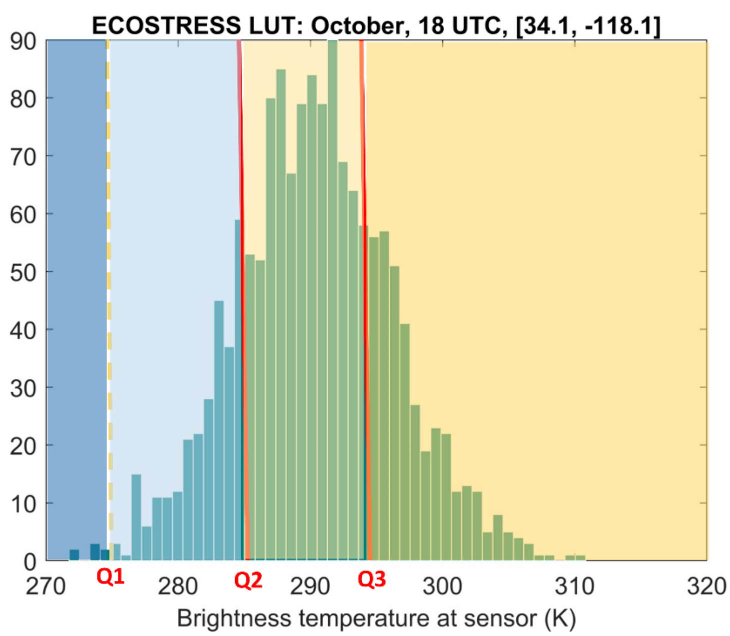

Figure 3: Example ECOSTRESS clear-sky brightness temperature (BT) distribution for the month of October at 18 UTC for location 34.1 N, -118.1 (JPL, Pasadena). Cloud confidence levels are determined from thresholds set at Q1, Q2 and Q3 (see text for details).

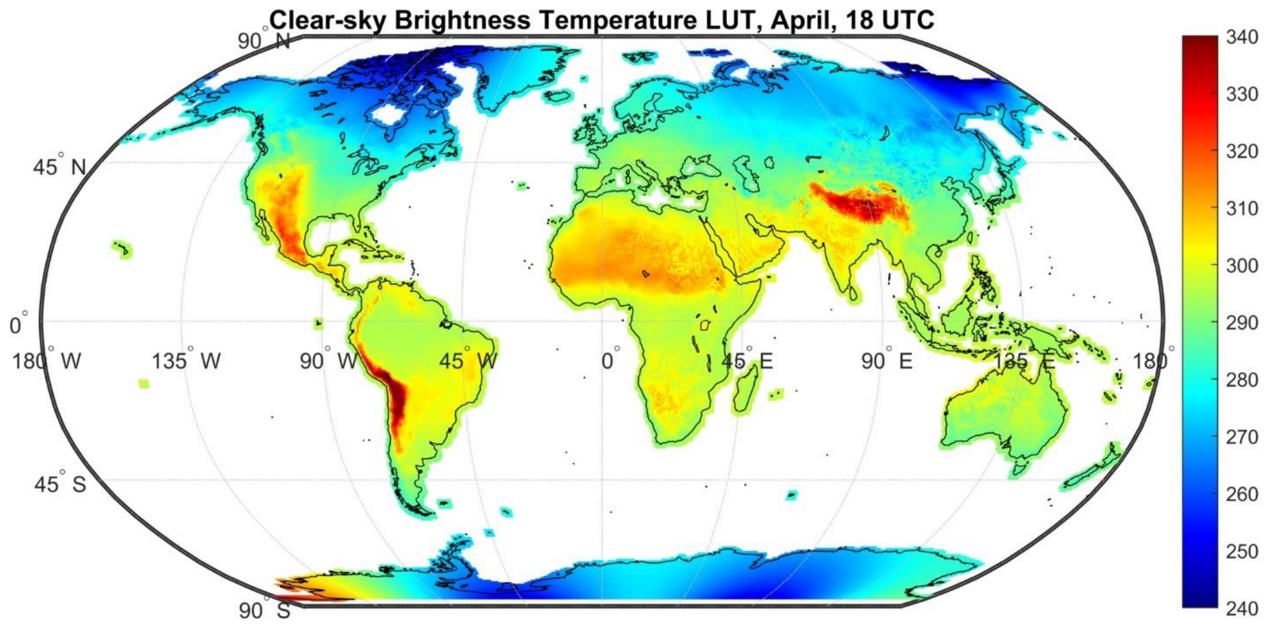

Figure 4: Example ECOSTRESS clear-sky brightness temperature (BT) climatology Look Up Table (LUT) for April at 18 UTC. SBG observed BT's during April at or near 18 UTC that fall below these values are considered cloudy.

The first confidence level is determined by Q1 and is used to find confident cloudy pixels:

$$Q1 = Q2 - 1.5 \times IQR$$

Where $IQR = Q3 - Q2$, Q2 is the 25th percentile and Q3 is the 75th percentile. Then any pixels with brightness temperatures less than Q1 are considered to be confident cloudy pixels. The second confidence level, probably cloudy pixels, is determined as pixels with brightness temperatures falling between Q1 and Q2. The third confidence level, probably clear pixels falls between Q2 and Q3 and lastly the fourth confidence level, confident cloudy pixels, are pixels with brightness temperatures greater than Q3.

Implementation of the cloud mask involves interpolating the global clear-sky brightness temperature Look Up Table (LUT) (see Figure 3 for ECOSTRESS) for each confidence level onto each SBG scene using bilinear interpolation between surrounding GEOS5 grid points and a temporal interpolation between the 6-hourly analysis fields. Figure 4 shows an example of the ECOSTRESS global gridded LUT for the month of August at 18 UTC. Note that the thresholds are determined for ocean along coastal zones as well, with a 2 degree (~200 km) buffer along coastlines. For SBG observations over open ocean, the coastal values are extrapolated into open ocean. While this may introduce uncertainty, the primary science focus of SBG data is over land.

Figure 5 shows an example of interpolation of the global grid LUT onto an ECOSTRESS scene on 5 April, 2022 at 18:46 UTC consisting of cloud over high elevation areas in the Rocky Mountains, USA. Cloud over high elevation areas is a challenging condition due to varying lapse rates and the presence of snow/ice during wintertime. To refine the thresholds further over these regions, we adjust the LUT thresholds using a standard lapse rate of 6.5 K/km using the SBG DEM included in the Geolocation product for the elevation. For this particular case, pixels with observed brightness temperatures less than the LUT values are considered confident cloudy, since the LUT shown here represents the Q1 confident cloudy threshold.

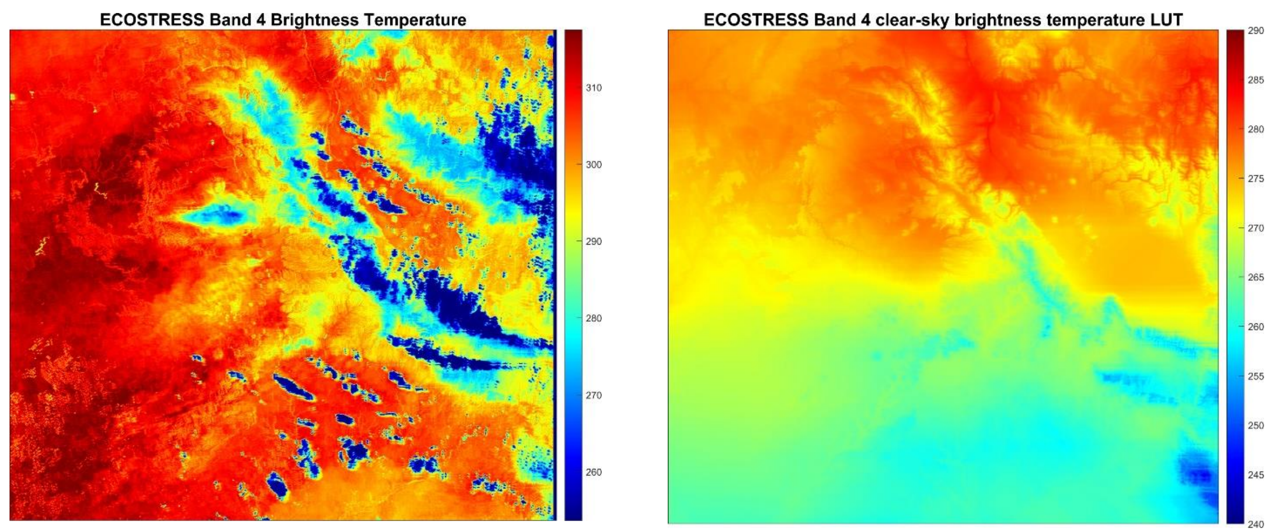

Figure 5: Example ECOSTRESS observed brightness temperature (BT) in band 4 (left) and spatially and temporally interpolated BT LUT (for Q1 confidence threshold) onto the SBG scene on 5 April, 2022 at 18:46 UTC.

4.2 Cloud mask confidence flags

The cloud product will contain two masks, a cloud confidence mask, and final estimated cloud mask. Users can interpret these data sets as follows:

1. Cloud_confidence contains the results of the brightness temperature LUT test with confidence levels set according to three threshold levels described above
    a. 0 = confident clear
    b. 1 = probably clear
    c. 2 = probably cloudy
    d. 3 = confident cloudy
2. Cloud_final contains a final cloud mask (1=cloud, 0=clear) based on the following criteria:
    a. For elevations < 2km, cloud = probably cloud + confident cloudy pixels
    b. For elevations >2km, cloud = confident cloudy pixels

Users can interpret the confidence levels and estimation of the final cloud mask as they wish, but the generalized rationale for the above logic is that mountainous areas with higher elevation will have larger uncertainties in the cloud mask due to the presence of snow/ice and effects of shading and varying temperature lapse rates. As a result only confident cloudy pixels are classified as cloud. For low lying regions using both probably and confident cloudy pixels provided a good balance between false positive and false negative cloud errors. If the user has zero tolerance for any nearby or possible cloud, then only confident clear pixels should be used, similarly if some cloud can be tolerated, then only confident cloudy pixels should be used.

Figure 6 and 7 show results of the Cloud_confidence and Cloud_final masks for an ECOSTRESS scene shown in Figure 9. Note that areas classified as probably cloud in the confidence mask are likely clear areas at higher elevations. For this reason, only the confident cloudy mask should be used to screen for cloud pixels. These thresholds are set so that in snow/ice conditions only confident cloudy pixels should be trusted as being cloud. The final cloud mask in Figure 7 is based on criteria 2b above, and the presence of cloudy pixels shows high correlation with the coldest brightness temperatures (likely cloud) in Figure 9.

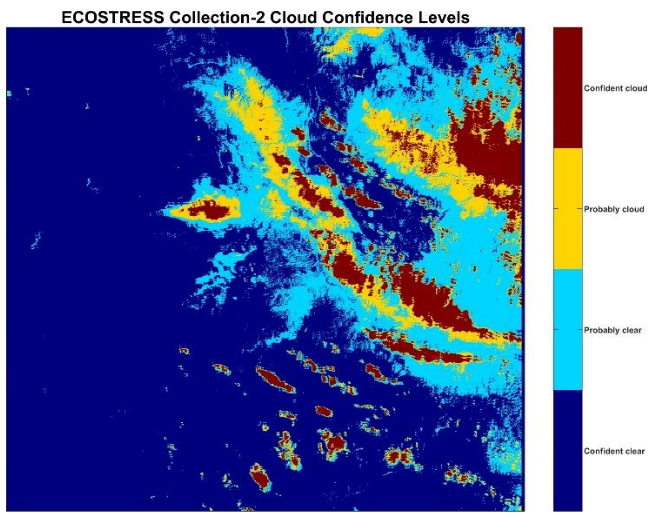

Figure 6: ECOSTRESS cloud confidence flag for a scene on 5 April, 2022 at 18:46 UTC.

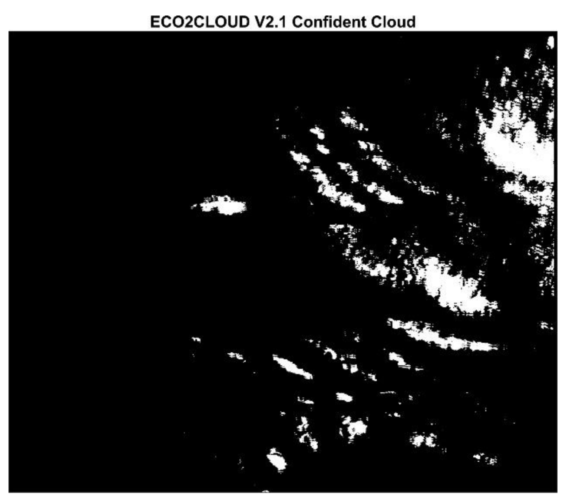

Figure 7: ECOSTRESS final cloud mask for a scene on 5 April, 2022 at 18:46 UTC.

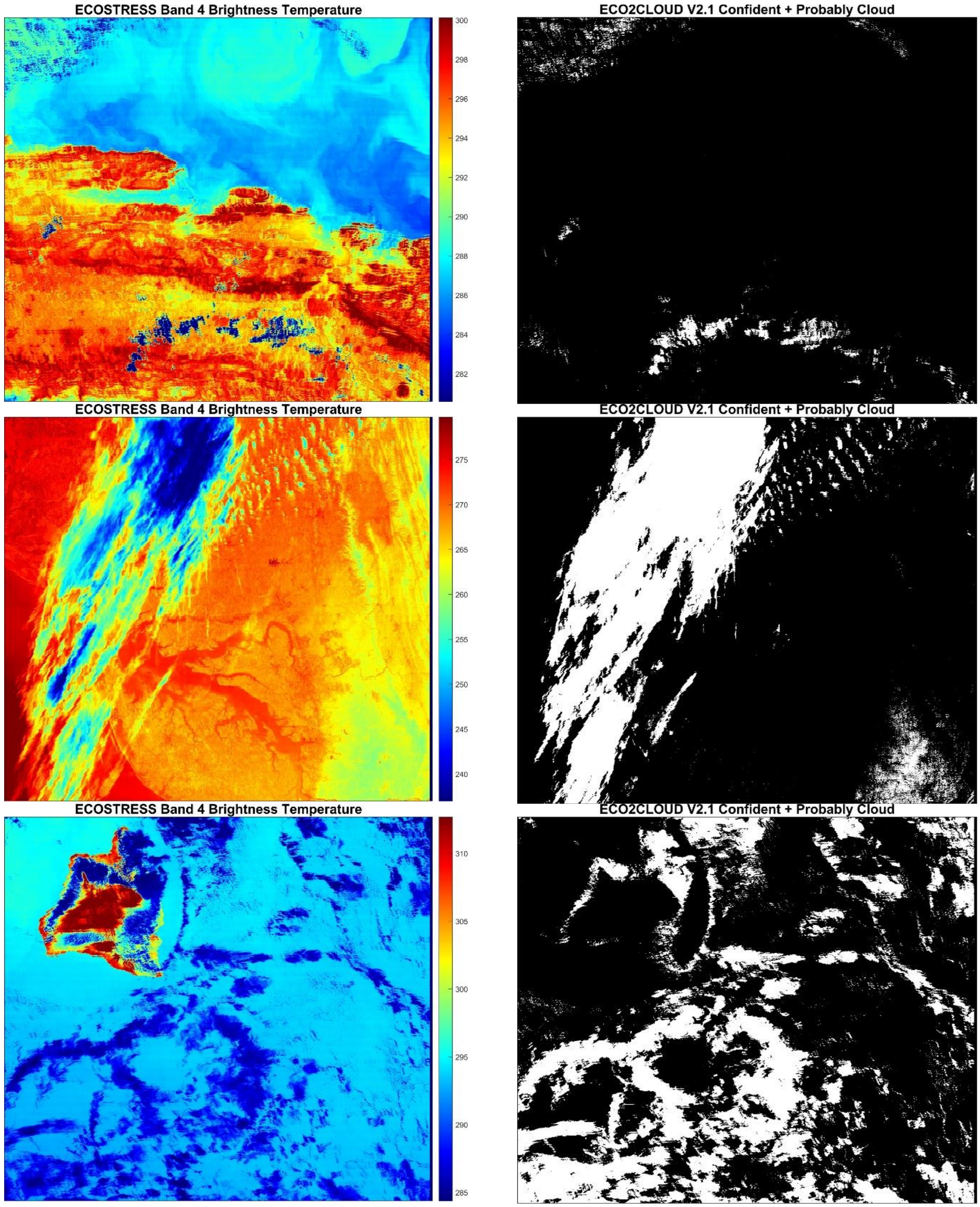

Figure 8: Further examples of the ECO2CLOUD v2.1 product (right) compared to ECOSTRESS band 4 brightness temperatures (left, cloud = cooler temps, blues and greens) for a wide variety of different types of scenes: (top) a very hot scene over Central valley with cooler coastal region, (middle) a very cold scene over Chesapeake bay during winter, and (bottom) a scene with mostly ocean surrounding Kuai, Hawaii.

5 Scientific Data Set (SDS) Variables

The SBG L2 Cloud Mask product will be archived in Hierarchical Data Format 5 - Earth Observing System (HDF5-EOS) format files. HDF is the standard archive format for NASA EOS Data Information System (EOSDIS) products. The L2 Cloud files will contain global attributes described in the metadata, and scientific data sets (SDSs) with local attributes. Unique in HDF-EOS data files is the use of HDF features to create point, swath, and grid structures to support geolocation of data. These structures (Vgroups and Vdata) provide geolocation relationships between data in an SDS and geographic coordinates (latitude and longitude or map projections) to support mapping the data. Attributes (metadata), global and local, provide various information about the data. Users unfamiliar with HDF and HDF-EOS formats may wish to consult Web sites listed in the Related Web Sites section for more information.

Table 4 details the data sets included in the L2_CLOUD output. Users can interpret the data sets as follows:

1. Cloud_confidence contains the results of the brightness temperature LUT test with confidence levels set according to different threshold levels: 0 = confident clear, 1 = probably clear, 2 = probably cloudy, and 3 = confident cloudy.

2. Cloud_final contains a final cloud mask (1=cloud, 0=clear) based on the following criteria:

   c. For elevations < 2km, cloud = probably cloud + confident cloudy pixels

   d. For elevations >2km, cloud = confident cloudy pixels

5.1 Scientific Data Sets (SDS)

Table 4. The SDSs in the SBG L2 Cloud product.

SDS	Long Name	Data type	Units	Valid Range	Fill Value	Scale Factor	Offset
Cloud_confidence	Brightness temperature LUT test	uint8	3=confident cloudy 2=probably cloudy 1=probably clear 0=confident clear	0-1	255	1	0
Cloud_final	Final cloud mask	uint8	1=cloud 0=clear	0-1	255	1	0

5.2 Attributes

Table 5. The metadata definition in the SBG L2 Cloud product.

Name	Type	Size	Example
Group	**L2 CLOUD Metadata**		
QAPercentCloudCover	Int	4	80
CloudMeanTemperature	LongFloat	8	231
CloudMaxTemperature	LongFloat	8	275
CloudMinTemperature	LongFloat	8	221
CloudSDevTemperature	LongFloat	8	0.45

6 References

Ackerman, S., Strabala, K.I., Menzel, P., Frey, R., Moeller, C.C., Gumley, L.E., Baum, B., Seemann, S.W., & Zhang, H. (2006). Discriminating clear-sky from cloud with MODIS algorithm theoretical basis document (MOD35), *Cooperative Institute for Meteorological Satellite Studies, University of Wisconsin-Madison, NOAA/NESDIS, version 5.0, October 2006*

Allen, R.G., Tasumi, M., & Trezza, R. (2007). Satellite-based energy balance for mapping evapotranspiration with internalized calibration (METRIC) - Model. *Journal of Irrigation and Drainage Engineering-Asce, 133*, 380-394

Anderson, M.C., Kustas, W.P., Norman, J.M., Hain, C.R., Mecikalski, J.R., Schultz, L., Gonzalez-Dugo, M.P., Cammalleri, C., d'Urso, G., Pimstein, A., & Gao, F. (2011). Mapping daily evapotranspiration at field to continental scales using geostationary and polar orbiting satellite imagery. *Hydrology and Earth System Sciences, 15*, 223-239

Borbas, E.E., Hulley, G., Feltz, M., Knuteson, R., & Hook, S. (2018). The Combined ASTER MODIS Emissivity over Land (CAMEL) Part 1: Methodology and High Spectral Resolution Application. *Remote Sensing, 10*

Bulgin, C.E., Sembhi, H., Ghent, D., Remedios, J.J., & Merchant, C.J. (2014). Cloud-clearing techniques over land for land-surface temperature retrieval from the Advanced Along-Track Scanning Radiometer. *International Journal of Remote Sensing, 35*, 3594-3615

Feltz, M., Borbas, E., Knuteson, R., Hulley, G., & Hook, S. (2018). The Combined ASTER MODIS Emissivity over Land (CAMEL) Part 2: Uncertainty and Validation. *Remote Sensing, 10*

Fisher, J.B., Tu, K.P., & Baldocchi, D.D. (2008). Global estimates of the land-atmosphere water flux based on monthly AVHRR and ISLSCP-II data, validated at 16 FLUXNET sites. *Remote Sensing of Environment, 112*, 901-919

Hulley, G.C., & Hook, S.J. (2008). A new methodology for cloud detection and classification with ASTER data. *Geophysical Research Letters, 35*, L16812, doi: 16810.11029/12008gl034644

Irish, R.R., Barker, J.L., Goward, S.N., & Arvidson, T. (2006). Characterization of the Landsat-7 ETM+ automated cloud-cover assessment (ACCA) algorithm. *Photogrammetric Engineering and Remote Sensing, 72*, 1179-1188

Markham, B.L., & Barker, J.L. (1986). Landsat MSS & TM Post-Calibration Dynamic Ranges, Exoatmospheric Reflectances & At-Satellite Temperatures. In, *EOSAT Landsat Technical Notes, No. 1.*

Merchant, C.J., Embury, O., Roberts-Jones, J., Fiedler, E., Bulgin, C.E., Corlett, G.K., Good, S., McLaren, A., Rayner, N., Morak-Bozzo, S., & Donlon, C. (2014). Sea surface temperature datasets for climate applications from Phase 1 of the European Space Agency Climate Change Initiative (SST CCI). *Geoscience Data Journal, 1*, 179-191

Saunders, R.W., & Kriebel, K.T. (1988). An Improved Method for Detecting Clear Sky and Cloudy Radiances from Avhrr Data. *International Journal of Remote Sensing, 9*, 123-150